ELSEVIER

Thermochimica Acta 255 (1995) 297–317

thermochimica acta

Suppression of crystallization in the binary system 1,2-propanediol–deuterium oxide. Comparison with light water as solvent

Patrick M. Mehl

Holland Laboratory, American Red Cross, 15601 Crabbs Branch Way, Rockville, MD 20855, USA
Transfusion Medicine Research Program, Naval Medical Research Institute, 8901 Wisconsin Avenue, Building 29, Bethesda, MD 20889, USA [1]

Received 16 July 1993; accepted 1 October 1994

Abstract

The solid–liquid phase diagram of the binary system D_2O–1,2-propanediol has been studied for concentrations up to 50% w/w. The homogeneous nucleation was also analyzed using an emulsification technique within the classical theory. The isothermal and non-isothermal crystallizations of ice were studied during warming for samples which vitrify during the initial cooling down below the glass transition. The thermal analysis was performed using the Johnson–Mehl–Avrami model extended to non-isothermal conditions. Comparisons are made with previous results from the binary system H_2O–1,2-propanediol. The suppression of crystallization during cooling is similar for both binary systems for concentrations in %mole/mole. The differences between melting and devitrification temperatures are also similar. The results do not indicate major differences between the crystallization kinetics with H_2O or with D_2O. Calculations of the kinetics parameters do, however, underline detailed differences. The suppression of the nucleation of ice is steeper for the D_2O system than for the H_2O system, even if the homogeneous nucleation temperatures are higher with D_2O than with H_2O. Estimates of the solid–liquid surface free energies are higher for the H_2O solvent than for the D_2O solvent and decrease as the 1,2-propanediol concentration increases. They cross over for a concentration close to 89% mole/mole solvent. For the isothermal and non-isothermal crystallization, the determination of the Avrami exponent is similar for the two solvents, with values of between 2.5 and 2 for solute concentrations higher than 37.5% w/w. However, D_2O presents higher absolute activation energy values than H_2O.

[1] Address for correspondence.

SSDI 0040-6031(94)02134-1

These variations confirm that the nucleation is better suppressed and the crystal growth less suppressed by addition of 1,2-propanediol in D_2O solutions than in H_2O solutions for dilute concentrations.

Keywords: Crystallization; Deuterium oxide; Nucleation; Phase diagram; Propanediol; SLE; Vitrification; Water

1. Introduction

An understanding of the suppression of ice crystallization in aqueous solutions is essential for the design of vitrification solutions for the purpose of cryopreservation of organs. The vitrification technique avoids ice crystal formation which is responsible for the major mechanical damage for cryopreserved organized tissues and organs [1]. This is the only actual technique which can be considered for long-term preservation of organs at very low temperatures. Previous studies have underlined the effect of 1,2-propanediol as a good vitrification agent in aqueous solutions and also as a good cryoprotectant for different biological systems [2,3]. In the present paper, the effect of the solvent is also investigated as a possible solution for the success of the vitrification technique. The substitution of the solvent by an analog solvent will bring more insight to the understanding of the solute/solvent interaction at low temperatures. This substitution of water (H_2O) by deuterium oxide (D_2O) has already been investigated in flushing solutions used for organ transplantation in rats. Fisher and co-workers have shown an improvement of the post-transplant recovery when water is substituted by D_2O [4,5]. D_2O is observed to behave as a good cryoprotectant for red blood cells [6]. Moreover, other advantages have been observed with D_2O: D_2O has been observed to stabilize proteins against either "cold" or warm denaturation [7–9], membranes, microtubules [6,10] and also to have a baroprotection effect on cells [11]; according to the melting and boiling point temperatures, D_2O is a more structured liquid than H_2O; D_2O liquid is therefore thought to have stronger hydrogen bonds than H_2O liquid [12]; a decrease in temperature increases the difference in the activation energies for the dielectric relaxation rates between D_2O and H_2O liquids [13] which may result in an increasing difference in the strength of hydrogen bonds between D_2O and H_2O liquids, the activation energies being higher for D_2O than for H_2O. All these considerations suggest D_2O as a possible solvent in the vitrification technique. The effect of D_2O on the suppression of ice crystallization by 1,2-propanediol is investigated here with the determination of the phase diagram and of the related kinetics for homogeneous nucleation and crystal growth at low temperatures, within the classical theories and adapted thermal analysis by calorimetry and cryomicroscopy. The results are compared with previous studies on the crystallization of ice in the binary system H_2O–1,2-propanediol [2], with a kinetics approach to the crystallization [14,15]. The dissociation of the effect of the solvent on the ice

nucleation and on the crystal growth is considered essential for the understanding of the crystallization kinetics.

2. Materials and methods

The samples were prepared with 1,2-propanediol (99%+, gold label from Aldrich), D_2O (100% D from Sigma) and diionized water. The concentrations are expressed in terms of %mole/mole to allow comparisons between solvents. Prior to the experiments, the samples were filtered through a 0.22 μm diameter filter to remove foreign particles.

2.1. Calibration

Phase transitions were recorded with a DSC-4 from Perkin-Elmer adapted to low temperatures down to −160°C. Samples weighed 6–20 mg. Warming and cooling rates ranged from 1 to "320"°C min^{-1}. Calibration of the DSC-4 was done on the melting temperature T_m of different pure compounds: methylcyclopentane (98% from Aldrich), $T_m = -142.4$°C; pentane (99%+ from Aldrich), $T_m = -129.7$°C; ethylcyclohexane (99%+ from Aldrich), $T_m = -111.3$°C; butylcyclohexane (99%+ from Aldrich), $T_m = -74.5$°C; and diionized water, $T_m = 0$°C. The temperatures and fusion heats were recorded as functions of the warming rate used, as usual [16]. The variation of the fusion temperature is a function of the warming rate with an approximate linear functions: $T_{read} = \alpha + \beta V$, where V is the warming rate, $\beta = 0.048 \pm 0.006$, a characteristic of the setting of the DSC-4, and α is the transition temperature at the limit $V = 0$°C min^{-1}. The temperature calibration allows corrections in the determination of the read transition temperatures to be made, and the estimate of the fusion heats for each compound gives an error of less than 3%.

2.2. Homogeneous nucleation

The determination of the nucleation temperatures was carried out using an emulsion technique with a 1:1 mole:mole ratio of methylcyclopentane and methylcyclohexane, with the addition of 4% w/w of SPAN 65 (Fluka) as surfactant. This emulsifiant solution and the sample solution were weighed and mixed together by passing them several times through a 26-gauge needle to form the emulsion, using a glass syringe to reach a mean value for the size of the droplets. This technique was developed by Rasmussen and MacKenzie for the study of homogeneous nucleation in aqueous solutions [17]. The size of the droplets was checked by cryomicroscopy monitored through a television set as previously described for the determination of nucleus density [14], except that the magnification was changed by a factor of 1500 from sample to television screen. The mean size of the major number of droplets which were assumed to participate in the homogeneous nucleation peak was estimated to be $v = 9 \times 10^{-18}$ m^3 within a factor 3 which corresponds to a reading

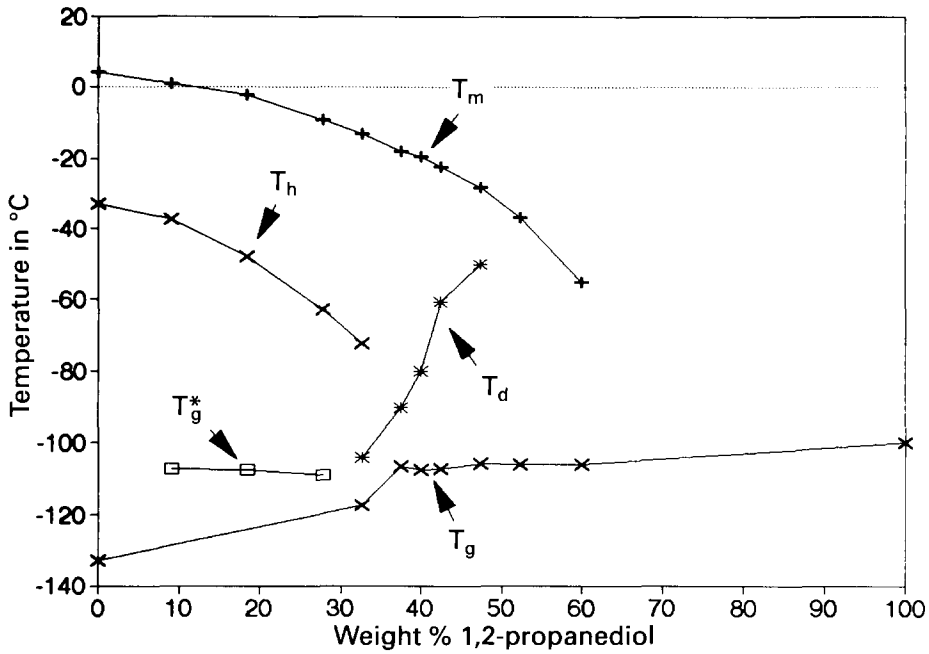

Fig. 1. Supplemented phase diagram of the binary system 1,2-propanediol–D_2O. The different temperatures are reported as: T_m, end of ice melting; T_h, onset of the homogeneous nucleation; T_g^*, glass transition of the residual amorphous material after ice crystallization; T_g, glass transition with no crystallization during the initial cooling; T_d, devitrification or crystallization during warming determined at the bottom of the crystallization peak. Homogeneous nucleation temperatures were determined using an emulsion technique with a cooling rate of 2.5°C min^{-1}. The other temperatures were determined in bulk samples during warming at 2.5°C min^{-1} after cooling at "320°C min^{-1}". The temperatures are corrected with the calibration of the DSC-4.

error of 1 mm on the screen. Successive cooling and warming can be done without changing the size of the emulsions, as reported by Angell et al. [18,19]. The kinetics for the homogeneous nucleation was then analyzed using the method reported below. Several cooling rates were used, from 2.5 to 20°C min^{-1} for D_2O, and only 2.5°C min^{-1} for H_2O. Higher cooling rates were not considered due to possible thermal conduction lag. Even if calibration during cooling was accurate, it was assumed that the kinetics of nucleation was the same for the same sample at different cooling rates, with the absolute calibration in temperature at zero cooling rate being identical to that of the warming rate (see Fig. 1). This assumption was applied to 9.09% w/w 1,2-propanediol in D_2O for the determination of the slope of the error versus cooling rate curve. This slope was then used for the determination of the error for the other studied concentrations to limit the effect of ice crystal growth on the determination of the ice nucleation kinetics. Indeed, the recording of the ice nucleation peak is due to the growth of the ice crystal within the droplet as soon as the ice nucleus is formed. This assumes that the thermal range of ice crystal growth is strongly overlapping with that of homogeneous ice nucleation.

2.3. Crystallization kinetics

The crystallization during cooling and warming was recorded for analysis, and the quantity of ice formed in the solutions was also analyzed. Isothermal and non-isothermal crystallization were investigated for various concentrations of 1,2-propanediol in D_2O and compared with previous data for 1,2-propanediol in H_2O. The chosen concentrations were those where crystallization was not recordable within the sensitivity of the DSC-4. TADS and DSCI software were used for the analysis of the crystallization kinetics and the determination of the different parameters within the Johnson–Mehl–Avrami theoretical model under isothermal conditions, as usual [14,15,20,21]. The non-isothermal data were analyzed using a modified equation derived from the isothermal JMA model [15] presented in the next section.

3. Analysis methods

3.1. Nucleation kinetics during cooling

The nucleation was analyzed using the classical method of Turnbull [22]. In the DSC-4, homogeneous nucleation occurs by spontaneous formation of clusters which might be stable or unstable. The DSC-4 records the crystal growth of the stable nuclei within the droplets. It was assumed that only one stable nucleus will induce crystallization inside each droplet. The case of multiple nuclei formation within one droplet was excluded. The thermal curve during cooling gives the power dQ/dt given to the sample to maintain it at the same temperature as the reference. Assuming that the droplets have the same mean volume, the heat released at the temperature T by the crystallization of dN droplets induced by dN formed nuclei during the time dt is

$$dQ = q\ dN \tag{1}$$

with q being the mean heat release by crystallization of one droplet. The rate of formation of the nuclei also depends on the initial potential nuclei sites which is the number of remaining unfrozen droplets at temperature T, $N(T)$. This number can be accessed by calculating the heat release from the temperature T until the end of the crystallization peak, which is

$$Q_{\text{rest}} = qN(T) \tag{2}$$

Then by taking the ratio

$$dQ/Q_{\text{rest}} = dN/N \tag{3}$$

it is possible to have access to the nucleus formation rate. The nucleation rate J is given by

$$J = [dN/dt]/V \tag{4}$$

where V is the volume of the remaining unfrozen sample. If τ is the ratio N/V, τ is also $1/v$ where v is the mean volume of one droplet, assuming the formation of one nucleus per droplet. Therefore $V = Nv$ and J becomes equal to

$$J = [dN/dt]/[Nv] \tag{5}$$

The experimental data supply Jv

$$Jv = [dQ/dt]/Q_{rest} \tag{6}$$

The classical nucleation theory [23] indicates that the nucleation rate can be expressed by

$$J[T] = (A/\eta) \exp[B/F(T)] \tag{7}$$

with

$$F(T) = [T/T_m]^3[1 - (T/T_m)]^2 \tag{8}$$

as a temperature-dependent variable, A a constant, η the viscosity of the liquid, and

$$B = 16\pi\sigma^3/3kT_m H_f^2 \tag{9}$$

where σ is the interface solid–liquid free energy, T_m the melting temperature, k the Boltzmann constant, and H_f the molar heat of fusion [22]. The factor $16\pi/3$ in the expression for B is related to the shape of the nucleus which is assumed to be spherical. This assumption can be justified from the observation of cubic ice formation before growth of hexagonal ice [24,25]. Therefore, plots of the natural logarithm $\ln(Jv)$ versus $F(T)$ theoretically give lines which can be used for the determination of the different parameters. These different parameters are then analyzed as functions of the solute concentration. These calculations did not take into account the temperature dependence of the viscosity.

3.2. Isothermal crystallization

The isothermal conditions were analyzed within the JMA theoretical model where the crystallization fraction is related to the time exposure t by

$$X = 1 - \exp[-(Kt)^n] \tag{10}$$

with n the Avrami exponent, K the kinetics constant, which is assumed to have an Arrhenius dependence with the temperature

$$K = K_0 \exp[-A/T] \tag{11}$$

with an apparent activation energy A expressed in K units. The second derivative of Eq. (10) gives

$$d^2X/dt^2 = (1 - X)K^n t^{n-2} n[(n - 1) - n(Kt)^n] \tag{12}$$

At the bottom of the isothermal crystallization peak, at $t = t_{max}$, this second derivative is null. Then

$$Kt_{max} = [(n - 1)/n]^{1/n} \tag{13}$$

A was previously determined by plotting the logarithm of the exposure time t_{max} corresponding to the maximum crystallization rate versus $1000/T$ [14,15,20,21], as t_{max} is inversely proportional to the kinetics constant K. The other parameters were determined by plotting

$$\ln(-\ln(1-X)) = n[\ln(K) + \ln(t)] \quad (14)$$

as a function of the logarithm of the exposure time t. The Avrami exponents and the kinetics constants were determined after linear regression of the experimental data on the previous plots with the slope and the intersection at the origin. As reported previously [14,15], the cooling and warming rates have an effect on the nucleation kinetics. Therefore to complete the study, different cooling and warming rates were applied to study the effect of the different rates on the crystallization kinetics, and the time t_{max} was plotted on a logarithmic scale versus the sum of the inverse of the cooling and warming rates prior to the isothermal annealing at the different chosen temperatures, because the variation in K_0 depends on the nucleus density as indicated in classical theories [14,15]. This is related to the dependence of the kinetics constant K in the JMA model on the nucleation rate or the nucleus density [26]. Therefore, the previous plots are justified when the nucleation thermal range and the crystal growth thermal range are relatively well separated compared to the cooling and warming rates used, as observed for relatively high concentrated

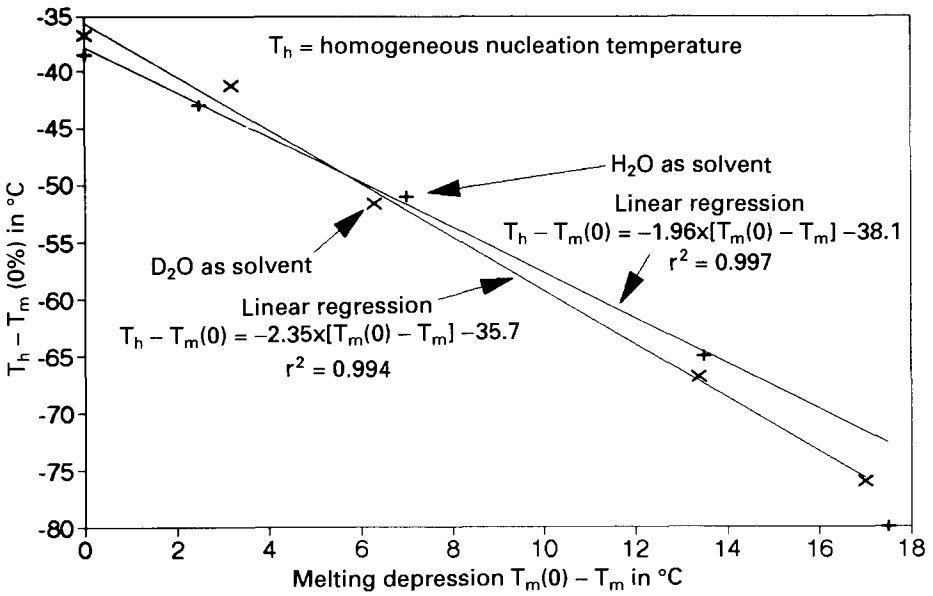

Fig. 2. Relative variations in the homogeneous nucleation temperature $T_h - T_m(0\%)$ versus the melting depression $T_m(0\%) - T_m$ for both binary system, 1,2-propanediol in D_2O and in H_2O. The lines represent the linear regression estimated for concentrations which do not achieve vitrification during cooling. This consideration avoids the effect of the viscosity on the nucleation kinetics.

aqueous solutions. However, when the extrapolated homogeneous nucleation temperature is well below the glass transition, the dependence becomes weaker and nucleation is determined by the concentration of heterogeneous sites for stabilization of the nuclei.

3.3. Non-isothermal crystallization

The non-isothermal conditions are more difficult to analyze. The crystallizable fraction as a function of the end of melting temperature T_m is required, as previously mentioned [15]. In this paper, a semi-integral/differential equation is deduced from the JMA model to be applied in non-isothermal conditions. The same parameters as for isothermal conditions are used. The calculations are processes with an algorithm for the determination of the quantity of heat released during the crystallization as a function of the scanning temperature. The equation of the kinetics is

$$dX(t) = nK^n t^{*(n-1)}[1 - X(t^*)]\, dt \tag{15}$$

and

$$X(t^*) = \left[Q_i + \int_{T_g}^{T} dQ \right] \Big/ Q^*_{max}(T) \tag{16}$$

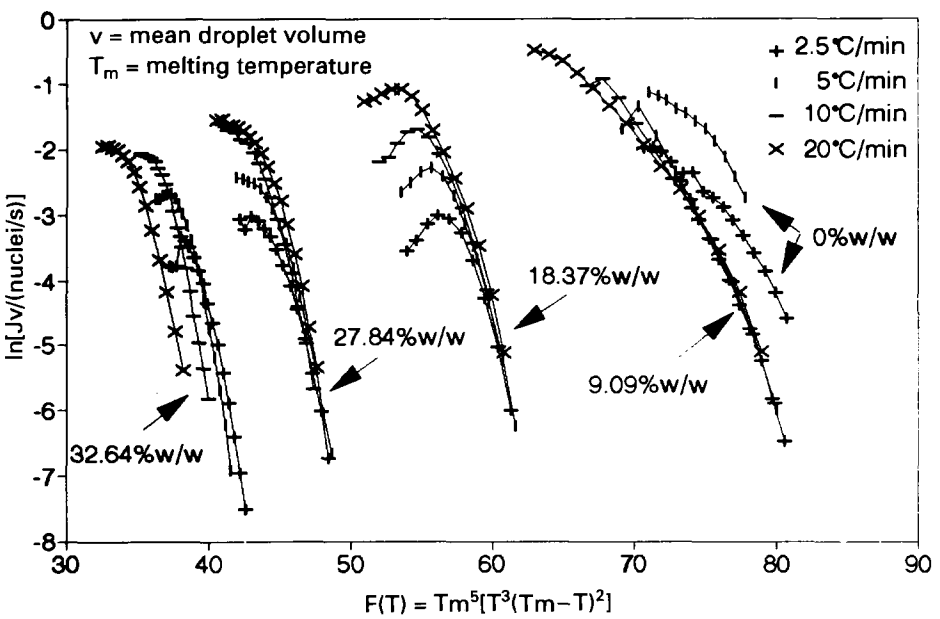

Fig. 3. Natural logarithms of the product of the nucleation rate J and the mean volume of the emulsion droplets versus the function $F(T) = T_m^5/[T^3(T_m - T)^2]$ for different concentrations of 1,2-propanediol in D_2O. Different cooling rates have been used to record the nucleation kinetics.

where K and n are the kinetics constant and the Avrami constant determined in isothermal conditions, respectively, and X is the volume ratio of the crystallized ice over the total crystallizable ice; X is approximated to the ratio of the corresponding heat of crystallization. Q_i is the heat of crystallization equivalent to the amount of ice already crystallized after cooling below the glass transition and is approximated to the heat of formation of the total stable nuclei which will grow during the subsequent warming. $Q^*_{max}(T)$ is the crystallization heat corresponding to a maximum quantity of formed ice at the temperature T. It should be noted that the times t^* and t are different: t is the scanning time of the thermal curve and t^* is the natural time of the material.

The crystallization during warming within the vitrified state is estimated using Eqs. (15) and (16) for the aqueous solutions which will vitrify within the cooling rate range of the DSC-4 and allow crystallization during the subsequent warming.

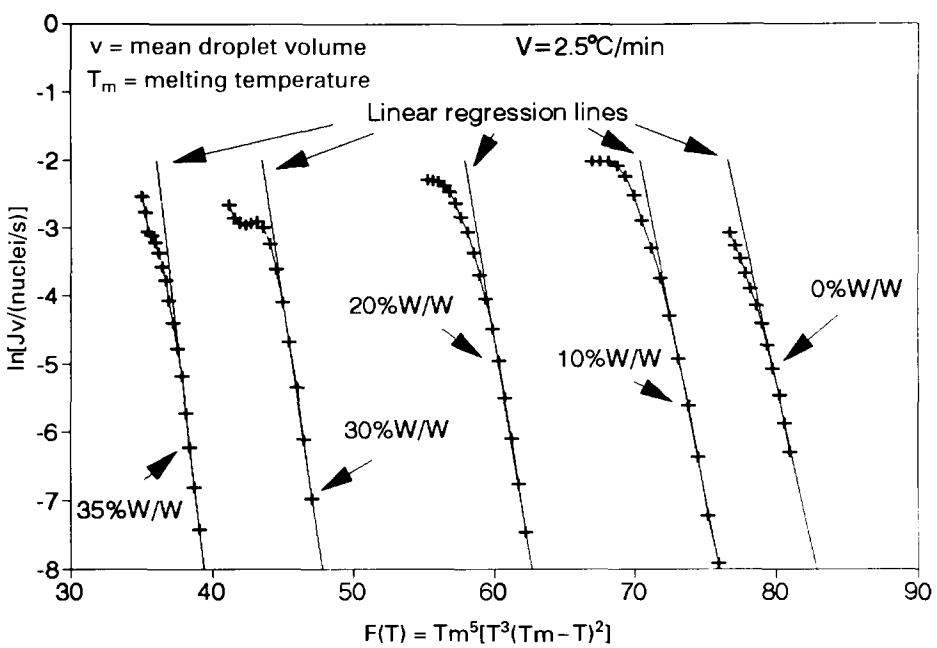

Fig. 4. Natural logarithms of the product of the nucleation rate J and the mean volume of the emulsion droplets versus the function $F(T) = T_m^5/[T^3(T_m - T)^2]$ for different concentrations of 1,2-propanediol in H_2O. Samples were cooled at 2.5°C min^{-1} only.

4. Results

4.1. Supplemented phase diagram

The different phase transitions observed on the recorded thermal curves are reported in Fig. 1. The end of melting, the homogeneous nucleation, the glass transition of the whole vitrified sample or of the amorphous residue after partial crystallization of ice, and the devitrification temperatures are recorded on cooling and warming at 2.5°C min^{-1}; these have been corrected with the calibration. No hydrate or eutectic formation is observed within the sensitivity of the DSC-4. The different transition temperatures are reported in Fig. 1. The homogeneous nucleation temperature is defined as the onset temperature of the exothermic crystallization peak observed during cooling of the emulsion sample. A comparison between H_2O [14] and D_2O solvents for the homogeneous nucleation temperature depression δT_h versus that of the melting temperature δT_m as the solute concentration increases is given in Fig. 2. As the solute concentration is above a threshold of 35–40% w/w of solute, the homogeneous nucleation temperature decreases more rapidly than the melting temperature with an increase in the solute concentration. As reported by other authors [17,23], a linear relationship between the two temperature depressions can be observed for low solute concentrations with

$$\delta T_h = 1.96\, \delta T_m \tag{17}$$

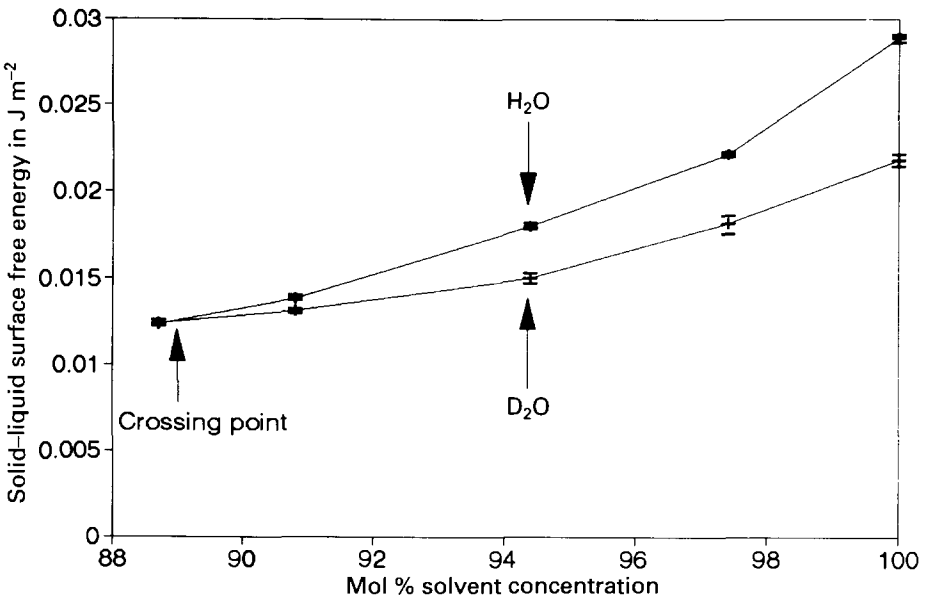

Fig. 5. Comparison of the liquid–solid surface free energy variations with the concentration of solvent when 1,2-propanediol is diluted in H_2O or in D_2O.

(without the homogeneous nucleation temperature for the 35% w/w 1,2-propanediol sample) for H_2O and

$$\delta T_h = 2.35\ \delta T_m \tag{18}$$

for D_2O. No nucleation is observed in emulsified samples of concentration higher than 37.5% w/w at cooling rates higher than 1°C min^{-1}. This suggests that the crystal growth thermal domain is at higher temperatures than that of the homogeneous nucleation.

4.2. Homogeneous nucleation kinetics

The nucleation rate Jv is reported on a logarithmic scale versus $F(T)$ as defined in the previous section (Fig. 3). For comparison, the nucleation with H_2O as solvent is also analyzed and the nucleation rate Jv is similarly reported in Fig. 4 with only a cooling rate of 2.5°C min^{-1}. The slope B is estimated and the solid–liquid interface free energy σ can be extracted from Eq. (9). Indeed, H_f^* and T_m are accessible, where H_f^* is the heat of fusion per gram of solution, and the determination of the molar mass for the liquid can be made from published data by the approximate determination of the density of D_2O or H_2O and 1,2-propanediol at low temperature using a quadratic form [27]. The surface solid–liquid free energy σ for the binary system 1,2-propanediol in either H_2O and D_2O was then

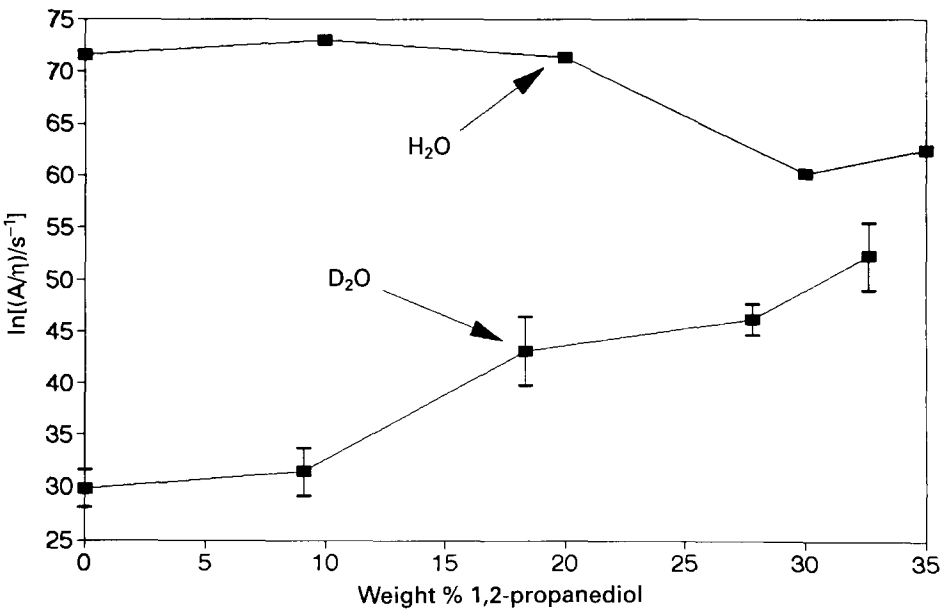

Fig. 6. Comparison of the variations of the preexponential term A divided by the viscosity with the concentrations of 1,2-propanediol, in the product Jv with H_2O or D_2O as solvent.

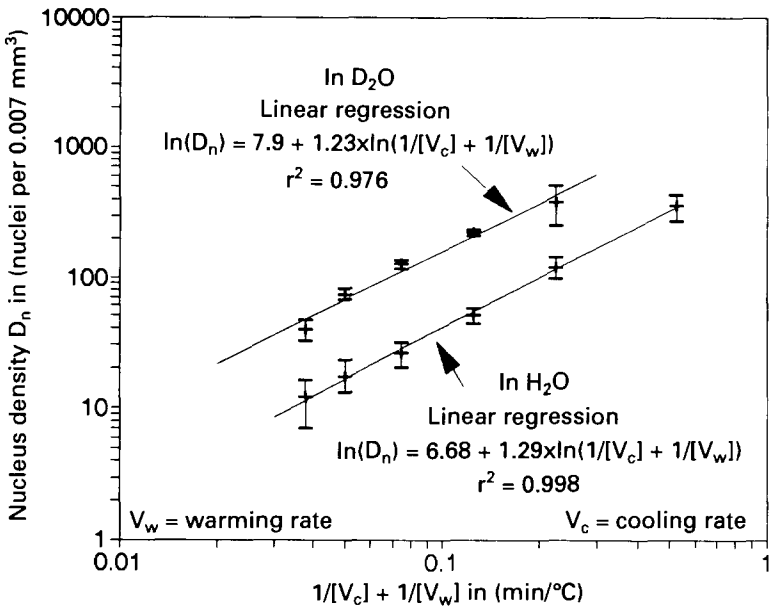

Fig. 7. Comparison of the dependence of the nuclei density determined by cryomicroscopy for 14.88% mole/mole 1,2-propanediol in D_2O or in H_2O, with the sum of the inverse of the cooling and warming rates.

calculated and is reported in Fig. 5 as functions of the molar concentration. The preexponential factor for the nucleation rate *Jv* is reported in the Fig. 6 with a similar droplet size distribution for the different solute concentrations as checked by cryomicroscopy. The diameter of the droplets has a mean value of 2.6×10^{-6} m, with a standard deviation of 0.7×10^{-6} m.

As reported previously, the thermal ranges for nucleation and crystal growth do not overlap for the experimental time scale for concentrations of 1,2-propanediol higher than 37.5% in D_2O. Therefore, the cryomicroscopy technique was used for these "vitrifiable" solutions. The nucleus density is reported for 39.95% w/w 1,2-propanediol in D_2O in Fig. 7 and compared with those previously published for 42.5% w/w 1,2-propanediol in H_2O [14]. The nucleus density is plotted against the sum of the inverse of the cooling rate and the warming rate which is proportional to the time spent by the liquid in the nucleation thermal range. The slope of the curve is estimated as 1.23 for D_2O and 1.29 for H_2O.

For intermediate concentrations, the homogeneous nucleation temperature is closer to the glass transition and the effect of the viscosity on the intrinsic crystal growth used in the emulsion technique to reveal the nucleation is not negligible. A more interesting observation is the lack of correlation of nucleation between adjacent crystallizing droplets. Indeed, each droplet crystallizes during cooling in a way that is independent of the state of its next neighbor. Moreover, as a droplet

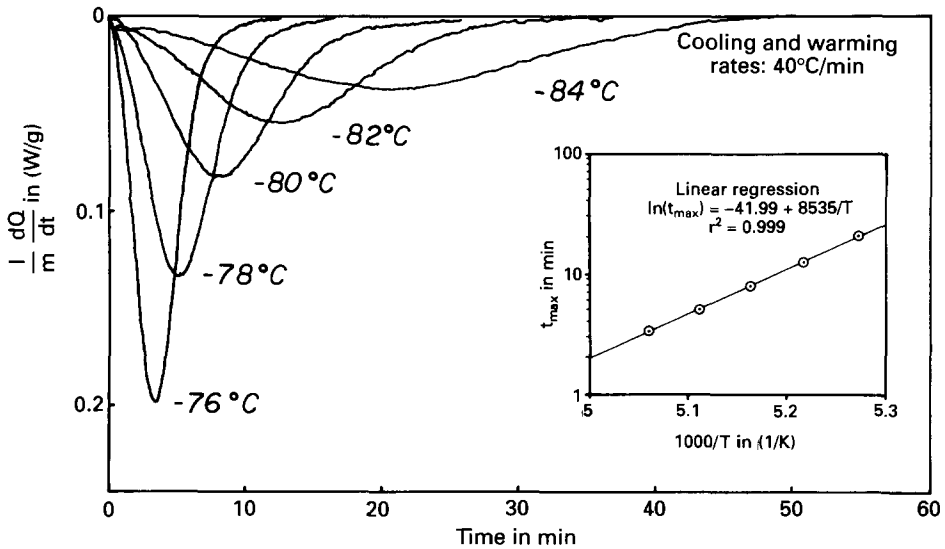

Fig. 8. Crystallization peaks in isothermal conditions for 39.95% w/w 1,2-propanediol in D_2O. In the inset graph, the time t_{max} corresponding to the maximum crystallization rate or at the bottom of the crystallization peaks is reported as an Arrhenius function of $1000/T$. The linear regression was performed and is reported in the inset graph. The slope is the apparent activation energy for the crystallization. The annealing temperatures reported on the peak sides are not corrected. They have been corrected for the inset graph.

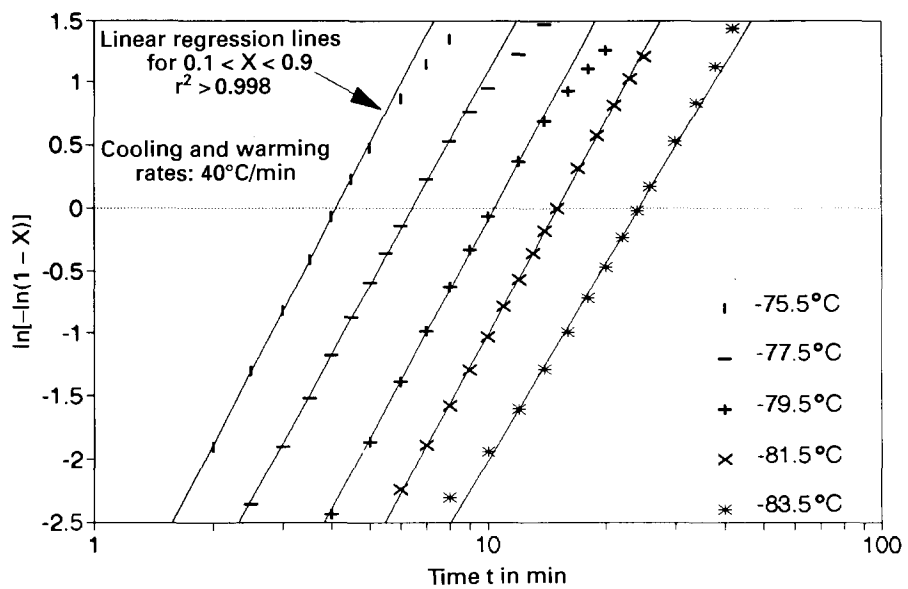

Fig. 9. $\mathrm{Ln}(-\ln(1-X))$, where X is the crystallized fraction at the temperature T, is drawn as a function of the annealing time t. The experimental conditions are those of Fig. 8. The linear regression allows the determination of the Avrami exponent and of the kinetics parameters.

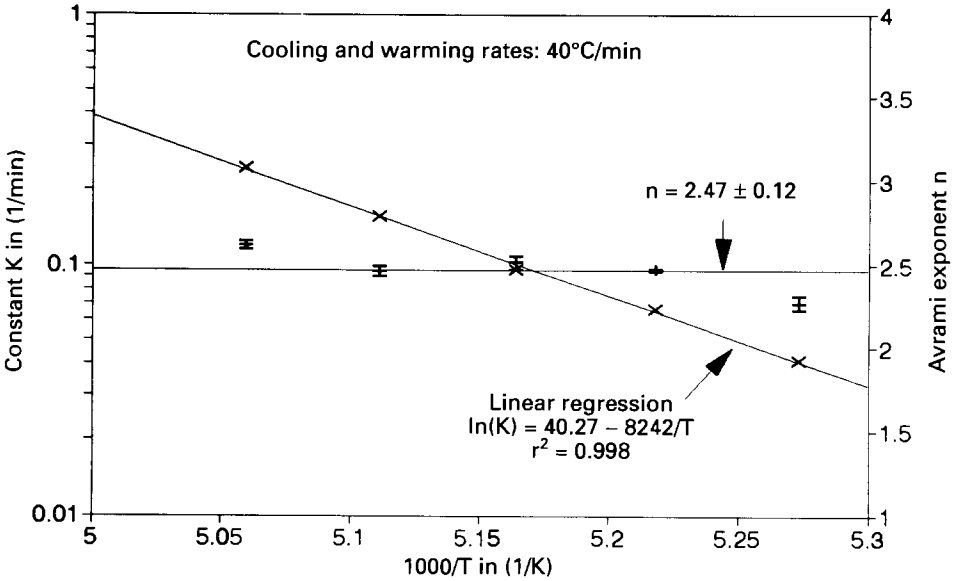

Fig. 10. Arrhenius representation of the kinetics constant $K(T)$ versus $1000/T$. The values of the Avrami exponents are also reported. The experimental conditions are those in Fig. 8.

crystallizes, it releases heat proportional to the size of the droplet. This heat will diffuse to the next neighbors which will become warmer than they would have been without the crystallized droplets. Therefore, the crystallization of one droplet will limit the nucleation within the next neighbors.

4.3. Isothermal crystallization

The isothermal results were analyzed within the JMA theoretical model. The recorded isothermal crystallization peaks (as reported for 39.95% w/w 1,2-propanediol in D_2O in Fig. 8) were used to determine the time of the maximum crystallization rate (bottom of the crystallization peak corresponding to $d^2Q/dt^2 = 0$), and the time variation of the crystallized fraction as a function of the temperature. The apparent activation energy is determined as the slope in Fig. 8 and the plot of $\ln(-\ln(1-X))$ versus $\ln(t)$, as reported in Fig. 9, gives the determination of the Avrami exponent and the kinetics function K as a function of the temperature at which the isothermal experiment was processed. As the constant $K(T)$ also depends on the thermal history, the effect of different cooling rates on the kinetics is shown in Fig. 10, as previously reported for the solution 42.5% w/w 1,2-propanediol in H_2O [14]. The apparent activation energy, the rate constant K and the Avrami exponent for 42.5% w/w 1,2-propanediol in H_2O are respectively 66.1 kJ mol^{-1}, 0.109 min^{-1} at $-84°C$, and 2.2 ± 0.2 [14]. This behavior is similar to that of the nucleation process. For higher concentrations of 1,2-propanediol in D_2O, the

Table 1
Heat of crystallization (cal per g of solution) versus cooling rates for different concentrations (%weight/weight and %mole/mole) of 1,2-propanediol. Comparison of the solvents H_2O (from Ref. [2] and this study) and D_2O

Solvent	%Solute		Cooling rates/°C min^{-1}							
	W/W	M/M	2.5	5.0	10	20	40	80	160	320
D_2O	18.37	5.58	32.9	–	33.1	–	33.6	–	–	–
H_2O [a]	20.00	5.58	33.0	–	32.4	32.9	33.7	33.1	–	–
D_2O	27.84	9.20	23.3	–	22.4	–	22.4	19.7	18.0	–
H_2O [a]	30.00	9.20	20.3		21.2	21.5	21.7	21.1	17.0	7.5
D_2O	32.64	11.30	18.9	–	19.1	14.3	0.9	0.2	0.0	
H_2O a	35.00	11.30	17.4	–	17.5	17.0	13.2	3.20	0.6	0.0
D_2O	37.50	13.62	14.6	13.5	10.3	1.1	0.0	0.0	0.0	0.0
H_2O a	40.00	13.52	13.2	–	4.9	1.3	0.0	0.0	0.0	0.0
D_2O	39.95	14.88	13.8	3.1	1.0	0.0	0.0	0.0	0.0	0.0
H_2O	42.50	14.88	10.9	2.2	0.5	0.0	0.0	0.0	0.0	0.0
D_2O	42.40	16.21	0.0	0.0	0.0	0.0	0.0	0.0	0.0	0.0
H_2O [a]	45.00	16.21	4.9	–	0.0	0.0	0.0	0.0	0.0	0.0
D_2O	47.37	19.13	0.0	0.0	0.0	0.0	0.0	0.0	0.0	0.0
H_2O a	50.00	19.13	0.0	0.0	0.0	0.0	0.0	0.0	0.0	0.0

[a] Results from Boutron and Kaufmann [2].

dependence of the time t_{max} with the cooling and warming is weaker, which can indicate a saturation of heterogeneous nucleation sites for the present experimental conditions.

4.4. *Non-isothermal crystallization*

The effect of the cooling and warming rates on the crystallization is reported in Table 1 and in Fig. 13, below. The amount of crystallization as a function of the cooling rate in Table 1 shows the effect of the solute concentration on the ability to suppress crystallization. The suppression during cooling in the diluted aqueous solutions is linked to the efficiency of the heterogeneous nuclei present in the solutions. As soon as the first or the first few heterogeneous nuclei are formed, crystal growth occurs quickly due to the low viscosity of the liquid at this temperature. Fig. 11 reports the difference between the temperature of melting T_m and the devitrification temperature T_d with a comparison between D_2O and H_2O as solvents. No large discrepancy exists between the two solvents. Even if T_m is suppressed by a few degrees from D_2O to H_2O, the effects of 1,2-propanediol concentrations and cooling rates on the suppression of ice crystallization are comparable.

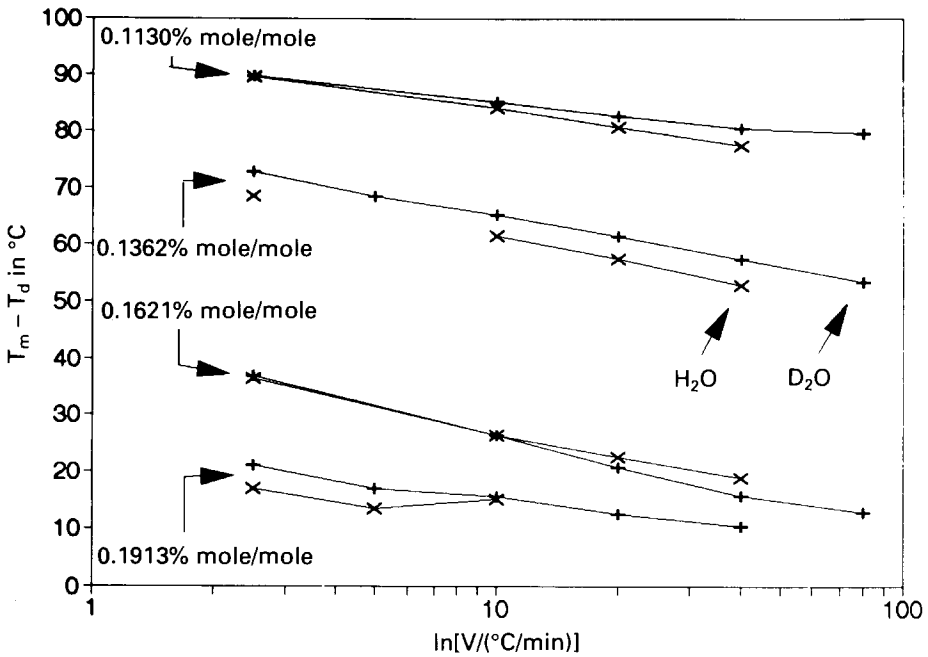

Fig. 11. Variations in the difference $T_m - T_d$ as a function of the natural logarithm of the warming rate for concentrations of 1,2-propanediol, allowing vitrification during cooling.

The maximum amount of crystallized ice is a function of the melting temperature T_m. It can also be related to the isothermal crystallization through the JMA theoretical model, as done for previous studies where isothermal crystallization took place at temperatures close to T_m. A slowing down of the crystallization was observed due to a limitation of the driving force for the crystallization which is the concentration difference between the equilibrium concentration after complete crystallization at the temperature T and the initial concentration.

4.5. Relation between isothermal and non-isothermal crystallization

A recent equation has been developed that uses directly the JMA parameters determined under isothermal conditions for the calculation of the devitrification peaks in non-isothermal conditions [15]. This method has been applied to 42.5% w/w 1,2-propanediol in H_2O with good results and was applied here for the present binary system for different solute concentrations. The parameters determined in isothermal conditions were placed in the differential system to be solved. The devitrification peak is calculated as a function of the warming rate assuming that the ice nucleation during cooling occurs for the vitrified samples without any growth of the nuclei. This assumption holds for concentrations with homogeneous nucleation temperatures close to that of the glass transition.

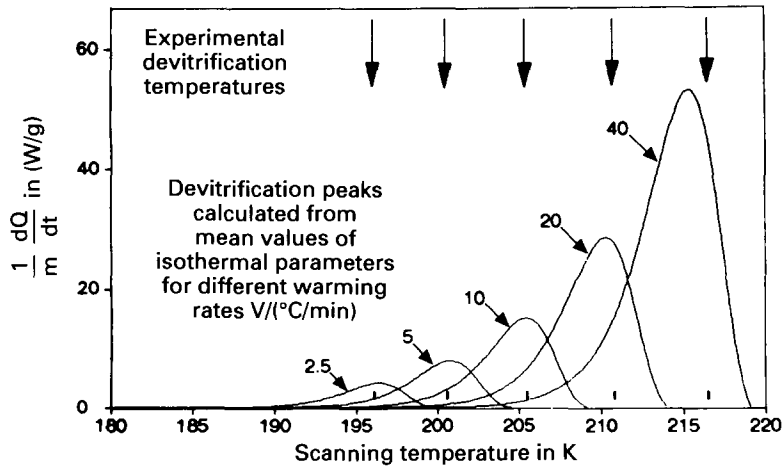

Fig. 12. Calculated devitrification peaks for 39.95% w/w 1,2-propanediol in D_2O. For comparison, the experimental devitrification temperatures are reported. The calculations were performed directly with the isothermal parameters.

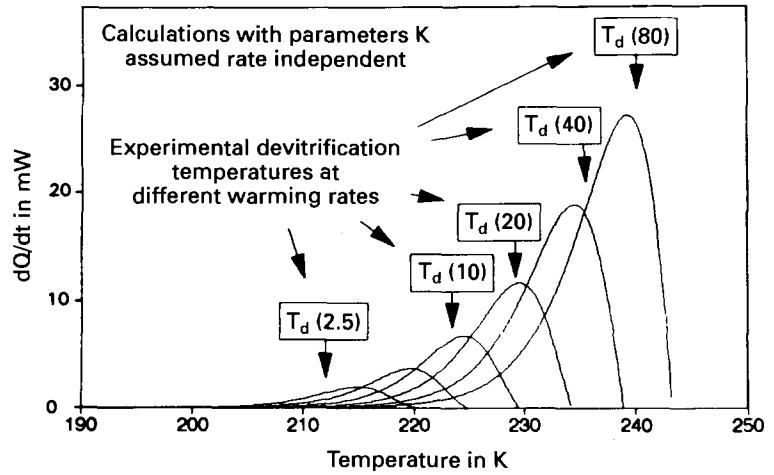

Fig. 13. Calculated devitrification peaks for 42.4% w/w 1,2-propanediol in D_2O. The calculations proceeded assuming that the constant K is weakly dependent on the warming rate.

The cooling and warming rates affect the kinetics of the crystallization as reported previously [14]. The main effect is on the nucleus density inside the material. Indeed, as reported in Fig. 10, the variation of the kinetics constant K depends on the time spent by the sample in the nucleation thermal range. However, for concentrations corresponding to homogeneous nucleation temperatures below the glass transition, this dependence is weaker for 42.5% w/w 1,2-propanediol in

D_2O with a critical exponent α close to 0 for $K[Dn]^z = \text{constant}$. Therefore, knowledge of the thermal variations of the nucleus density is important for the calculation of non-isothermal crystallization as anticipated by the model of Johnson–Mehl–Avrami. In Fig. 12, the calculated devitrification peaks are drawn showing a comparison with the experimental devitrification temperatures for 42.5% w/w 1,2-propanediol in D_2O. In contrast with 39.95% w/w 1,2-propanediol in D_2O, K_0 depends on the cooling and warming rates (Fig. 10); this dependence is taken into account in the calculations. The calculated peaks are reported in Fig. 13 with the experimental devitrification peaks.

5. Discussion

The supplemented phase diagram in Fig. 1 shows that for the binary system 1,2-propanediol–H_2O, no eutectic or hydrate forms. Crystallization is suppressed with solute concentrations higher than 11.3% mole/mole 1,2-propanediol (Table 1). For lower concentrations, after crystallization of ice during cooling, the remaining amorphous residue presents a glass transition T_g^* which is not constant but decreases slightly with the concentration. This is due to the crystallization process and the diffusion across the high solute concentration layer around the crystals. For lower concentrations, crystallization occurs at higher temperatures allowing a higher diffusion of water molecules through the high concentration layer, resulting in a more complete crystallization. When crystallization is not recorded, the sample is vitrified during cooling below the glass transition T_g. For 32.64% w/w 1,2-propanediol in D_2O, a sharp increase in the value of T_g is observed, as reported by Boutron and Kaufmann when H_2O is the solvent at the same molar concentration (35% w/w) [2]. Similar behavior is observed with H_2O or D_2O as solvents. The main difference is that the melting temperatures for the D_2O system are 4–5.5°C higher than for the H_2O system, by comparing Fig. 1 and the results in Ref. [2]. The comparison with the literature values in Ref. [2] also gives melting temperatures that are higher by 3.6 ± 0.8°C for D_2O than for H_2O. However, the glass transition T_g values are difficult to compare because different definitions have been used in their determination. However, the T_g values for the D_2O system are slightly higher, by less than 3°C, than those for the H_2O system [2].

An investigation of the comparison of the homogeneous nucleation temperatures in aqueous solutions with H_2O and D_2O as solvents has been reported for several salts such as LiCl by Angell et al. [19]. They have shown that the homogeneous nucleation is lowered in the same manner with H_2O and with D_2O. This is in accord with a general depression of the transition temperatures from D_2O to H_2O due to the change in the molecular weight of the solvent. The depression of T_h versus the depression of T_m, with the assumption that T_m is characteristic of the osmotic properties of the solute interacting with the solvent, shows that D_2O has a stronger effect on the suppression of the homogeneous nucleation than H_2O for the dilute concentrations. However, in the present experiment the concentrations are sufficiently high to allow the vitrification, therefore the effect of the viscosity is not

negligible and an inversion of the depression of the homogeneous nucleation is observed: more nucleation occurs with D_2O than with H_2O as recorded by cryomicroscopy. This can be explained by the difference between the melting and glass transition temperatures, which are lower for H_2O than for D_2O. The effect of the viscosity on the nucleation kinetics is therefore more efficient in H_2O than in D_2O. From the results of Henderson and Speedy [27] on the effects of pressure on the melting temperature, the melting temperature decreases more quickly for D_2O than for H_2O.

However, the different parameters for the crystallization in isothermal conditions for H_2O and D_2O are close. The suppression of the ice crystallization is very close for both binary systems, as reported in Table 1. Therefore, a macroscopic analysis of the suppression of the crystallization will lead to the conclusion that D_2O and H_2O have the same physical behavior at low temperatures. In fact, as previously discussed, the nucleation processes are different. The nucleation seems to begin at different temperatures and the kinetics are different. Therefore, the crystal growth for D_2O and H_2O must be different. As calculated for the different concentrations of 1,2-propanediol in D_2O, the activation energy for D_2O as solvent is higher than that of H_2O as solvent. For example with 14.88% w/w 1,2-propanediol, H_2O has an apparent activation energy of 66.1 kJ mol^{-1} and D_2O has a mean value of 69.8 kJ mol^{-1}. A higher apparent activation energy slows the crystallization rate. This shows that the crystal growth rate is lower for D_2O ice crystals than for H_2O crystals in vitrifiable concentrations. Therefore, in view of Table 1 and Fig. 11, it seems that a compensation between nucleation and crystal growth exists for concentrations higher than 11.30% mole/mole 1,2-propanediol. However, the results seem to differ in Fig. 11 for 13.62%, with higher devitrification temperatures for H_2O than for D_2O. These results cannot be explained at present as the values for H_2O are from Ref. [2].

The validity of the determination of the kinetics parameters for the crystallization in isothermal conditions was checked through the determination of the devitrification peaks under constant heating rate conditions. In Fig. 7, it is shown that the stabilization during warming of the nuclei formed during cooling is dependent on the history of the sample and will effect the kinetic constant K as predicted in the JMA theory. As the solute concentration increases, the dependence of K on the warming rate decreases due to a limitation of the nucleation, with a possible switch from homogeneous to heterogeneous nucleation predominance in the crystallization. Therefore, as reported in Figs. 12 and 13, the devitrification peaks have been calculated with the mean values of the isothermal parameters of crystallization with either the dependence of K_0 on the warming rate for 39.95% w/w or the independence of K_0 for 42.5% w/w 1,2-propanediol in D_2O. In these figures, the experimental devitrification temperatures have also been reported for a qualitative comparison between theory and experiment. It seems that the theoretical calculations give good agreements for the lower warming rates but diverge slightly for the higher warming rates, e.g. for 39.95% w/w 1,2-propanediol at 40°C min^{-1} the difference between experimental and calculated T_d is less than 1.5°C. A better fit can be obtained within the standard error of the values of the parameters determined

isothermally. The same observation has been made for 42.5% w/w 1,2-propanediol in H_2O [15], with good agreement but also with a difference which increases with the warming rate.

In the whole discussion, the fact that D_2O solvent, like H_2O, will be ionized has been ignored. Indeed, it is difficult to distinguish the effect of the different distribution of the deuterium atom on the solute molecules as part of the atomic exchange between solute and solvent as the steady state of acid–base equilibrium is reached. Therefore assuming that all –OH groups are transformed to –OD in 1,2-propanediol to give $DOCH_2–CHOD–CH_3$, then the concentration of solute will only increase by a multiplication factor of 78/76 (1.0263). Therefore the increase in the suppression of the crystallization can only be explained by a possible exchange of deuterium atoms from solvent to solute. This can explain the transient behavior for concentrations between 32.5% and 39.95%, where vitrification seems to be easier to achieve for D_2O than H_2O as solvent. However, deuterated 1,2-propanediol is not commercially available to check the importance at low temperature of the proton substitution on the vitrification or the suppression of ice formation.

6. Conclusions

The results show that in general, the two binary systems of 1,2-propanediol in H_2O and in D_2O show similar behaviors and physical properties on a macroscopic level. However, as D_2O forms stronger bonds than H_2O, suppression of the crystallization is more difficult. On a microscopic level, the kinetics of the crystallization are different. As D_2O presents stronger bonds, the nucleation rates for D_2O are higher than for H_2O. However, the nucleation suppression is higher for D_2O than for H_2O when 1,2-propanediol is added. The calculated surface liquid–solid free energies for D_2O and H_2O both decrease with the initial concentration of 1,2-propanediol and cross at a concentration close to that allowing vitrification in the DSC-4. However, this vitrification is subject to the sensitivity of the DSC-4 to detect the nucleation: nucleation cannot be recorded directly and must be analyzed indirectly with successive annealing experiments [28]. This method has been used in a vitrification solution which has been tested for the vitrification of rabbit kidneys for long-term cryopreservation [28].

However, it has been observed that D_2O has the advantage over H_2O of a lower crystal growth kinetics. For the purpose of cryopreservation of organs, the important factor is the crystal growth. It has been shown that the size of intracellular ice crystals might be deleterious for the cells above a threshold radius of 50–80 nm [29,30] which might also be dependent on the sensitivity of various cells; arguments have been presented on the non-effect behavior of the nucleus density on the possible survival of vitrified organs [31]. Therefore a lower crystal growth kinetics will lower the warming rates needed to limit the size of the ice crystals below the deleterious threshold value. Moreover, with the consideration of the other interesting properties of D_2O [4–11], D_2O could partially or totally replace H_2O in

vitrification solutions to solve actual problems in the vitrification technique, with or without pressure, for long-term preservation of organs at very low temperatures.

Acknowledgements

The author thanks Dr. H.T. Meryman for his continuous support. This study is supported by NIH-grant #GM 17959-21.

References

[1] G.M. Fahy, D.R. MacFarlane, G.A. Angell and H.T. Meryman, Cryobiology, 21 (1984) 407.
[2] P. Boutron and A. Kaufmann, Cryobiology, 16 (1979) 557.
[3] P. Boutron and F. Arnaud, Cryobiology, 21 (1984) 348.
[4] J.H. Fisher, G. Reifferscheidt, M. Fuhs, M. Wenzel and W. Isselhard, in D.E. Pegg, I.A. Jacobsen and N.A. Halasz (Eds.), Organ Preservation, Symposium of the Transplant. Soc., 1981, MTP, Lancaster, UK, 1982, pp. 199–203.
[5] J.H. Fisher, and P. Knupfer, Chir. Forum Exp. Klin. Forsch. 67, 79–84 (1984) 79.
[6] M. Wenzel, Naturwissenschaften, 64 (1977) 441.
[7] C. Heyde and M. Wenzel, Z. Naturforsch., 46 (1991) 789.
[8] S. Chapelle and E. Schoffeniels, Arch. Int. Physiol. Bioch., 80 (1972) 1.
[9] L.C. Antonino, R.A. Kautz, T. Nakano, R.O. Fox and A.L. Fink, Proc. Natl. Acad. Sci. USA, 88 (1991) 7715.
[10] D. Masland, in M. Zimmerman (Ed.), High Pressure Effects on Cellular Processes, Academic Press, New York, 1970, Chapt. 11, pp. 259–312.
[11] Y. Komatsu, K. Obuchi, H. Iwahashi, S.C. Kaul, M. Ishimura, G.M. Fahy and W.F. Rall, Biochem. Biophys. Res. Commun., 174 (1991) 1141.
[12] R.A. Kuharski and J. Rossky, J. Chem. Phys., 82 (1985) 5164.
[13] Y. Tada, M. Ueno, N. Tsuchihashi and K. Shimizu, J. Sol. Chem., 21 (1992) 971.
[14] P.M. Mehl, Thermochim. Acta, 203 (1992) 475.
[15] P.M. Mehl, Thermochim. Acta, 223 (1993) 157.
[16] P.M. Mehl, Thermochim. Acta, 213 (1993) 177.
[17] D.H. Rasmussen and A.P. MacKenzie, in H.H.G. Jellinek (Ed.), Water Structure at the Water–Polymer Interface, Plenum Press, New York, 1972, pp. 126–145.
[18] C.A. Angell, in F. Franks (Ed.), Water, A Comprehensive Treatise, Vol. 7, Water and Aqueous Solutions at Subzero Temperatures, Plenum Press, New York, 1982, pp. 1–81.
[19] C.A. Angell, E.J. Sare, J. Donnella and D.R. MacFarlane, J. Phys. Chem., 85 (1981) 1461.
[20] P.M. Mehl, Thermochim. Acta, 155 (1989) 187.
[21] P.M. Mehl, Cryobiology, 27 (1990) 378.
[22] D. Turnbull, Contemp. Phys., 10 (1969) 473.
[23] F. Franks, in F. Franks (Ed.), Water, A Comprehensive Treatise, Vol. 7, Water and Aqueous Solutions at Subzero Temperatures, Plenum Press, New York, 1982, pp. 215–338.
[24] P. Boutron and P. Mehl, J. Phys. Colloq. C1, Supp. 3, 48 (1987) 441.
[25] T. Takahashi, J. Cryst. Growth, 59 (1982) 441.
[26] J.W. Christian, in R.W. Cahn (Ed.), Physical Metallurgy, North-Holland, Amsterdam, 1965, pp. 443–539.
[27] S.J. Henderson and R.J. Speedy, J. Phys. Chem., 91 (1987) 3069.
[28] P.M. Mehl, Cryobiology, 30 (1993) 509.
[29] T. Takahashi, A. Hirsh, E.F. Erbe, J.B. Bross and R.J. Williams, Cryobiology, 23 (1986) 103.
[30] K. Shimida, Contrib. Inst. Low Temp. Sci. Ser. B, 19 (1977) 49.
[31] P.M. Mehl, Cryo-Lett., 7 (1993) 21.